

## A low onset voltage WORM type polymer memory based on functional PES

Jiyong Fang, Haibo Zhang, Wei Wei, Yunxi Li, Xigui Yue, Zhenhua Jiang

Alan G. MacDiarmid Institute, College of Chemistry, Jilin University, 2699 Qianjin street, Changchun 130012, People's Republic of China

Correspondence to: X. Yue (E-mail: yuexigui@jlu.edu.cn)

**ABSTRACT:** A high-performance polymer polyethersulfone (CN-Azo-PES), with a flexible ethoxyl linkage between the azobenzene chromophore side chain and the PES backbone, has been designed and successfully synthesized for an application in a WORM type memory device as an active polymer layer. CN-Azo-PES has excellent thermal properties with  $T_g$  of 151°C and the degradation temperature higher than 373°C, which can contribute to a better performance of the device. The device based on CN-Azo-PES exhibits a write-once read-many (WORM) type memory performance with an onset voltage as low as  $-1.0$  V and an ON/OFF current ratio higher than  $10^2$  at a reading voltage of 0.4 V. Moreover, the data can be maintained for longer than  $4 \times 10^5$  s once written and can be read for more than 400 cycles under a reading voltage of 0.4 V. Thus CN-Azo-PES can serve as an energy saving memory material in the data storage field of next generation. © 2015 Wiley Periodicals, Inc. *J. Appl. Polym. Sci.* **2015**, *132*, 42644.

**KEYWORDS:** grafting; stimuli-sensitive polymers; thermoplastics

Received 17 March 2015; accepted 21 June 2015

DOI: 10.1002/app.42644

### INTRODUCTION

Nowadays, thanks to the amazing success of information technology industry (IT), organic polymer electrical memories have now been widely investigated as a fascinating candidate in the future data storage field, for their outstanding advantages of rich structure flexibility, superior solution processability, good scalability, and three-dimensional stacking capability, compared with the traditional inorganic semiconductor-based memories.<sup>1</sup> Therefore, a wide range of novel polymeric materials with electrically bistable behaviors have been reported recently, for instance, polyimides,<sup>2–5</sup> polymer, and graphene nanocomposites,<sup>6–8</sup> polymer and nanoparticles composites,<sup>9–11</sup> poly(N-vinylcarbazole) (PVK),<sup>12</sup> conjugated polymers,<sup>13,14</sup> hyperbranched polymer with pyrazoline moieties,<sup>15</sup> and so on. Besides, being completely different from the silicon-based devices which store data by encoding “0” and “1” as the amount of charge stored in the cells of the memory device, organic polymeric memories store information through two bistable resistance changes, that is, low-conductivity state and high-conductivity state, in response to an external electric field.<sup>1,16</sup>

However, to the best of our knowledge, though several kinds of polymer have been developed for memory usage, it is still an enormous challenge to apply polymer electronic memory in the laboratories to the industry because of many influencing factors, such as the thermal performance of the synthetic materials, the

device fabrication technology, the material design strategy (mechanism) and so on. Among these factors, the thermal properties and the material design strategy are crucial because outstanding thermal stability can make great contributions to a better performance of the devices. The decomposition of the materials induced by the thermal and the electric field in the process of memory storage can be avoided subtly. An exact material design strategy based on a certain mechanism will help to rapidly enlarge the family of polymer with the property of electrical bistability behavior, though it is hard and troublesome to design such kind of memory material. Recently, because of the superior thermal and mechanical properties, dimensional stability, and high chemical resistance, polyimides have gained increasing attention in recent publications.<sup>4,17,18</sup> However, as a thermosetting plastic, PIs have a relatively poor solubility in common solvents and poor processability which are undesirable in the fabrication of the memory device. Great efforts have been made to improve the solubility. For instance, some special monomers like 4,4'-hexafluoroisopropylidenediphthalic anhydride (6FDA), or some other fluorinated monomers are used, which are either poisonous in the synthetic procedure or difficult to synthesize.<sup>3</sup> Therefore, it is meaningful and necessary to exploit polymer electronic memories based on other polymers which have excellent thermal and chemical stabilities like polyimides according to a certain memory mechanism.

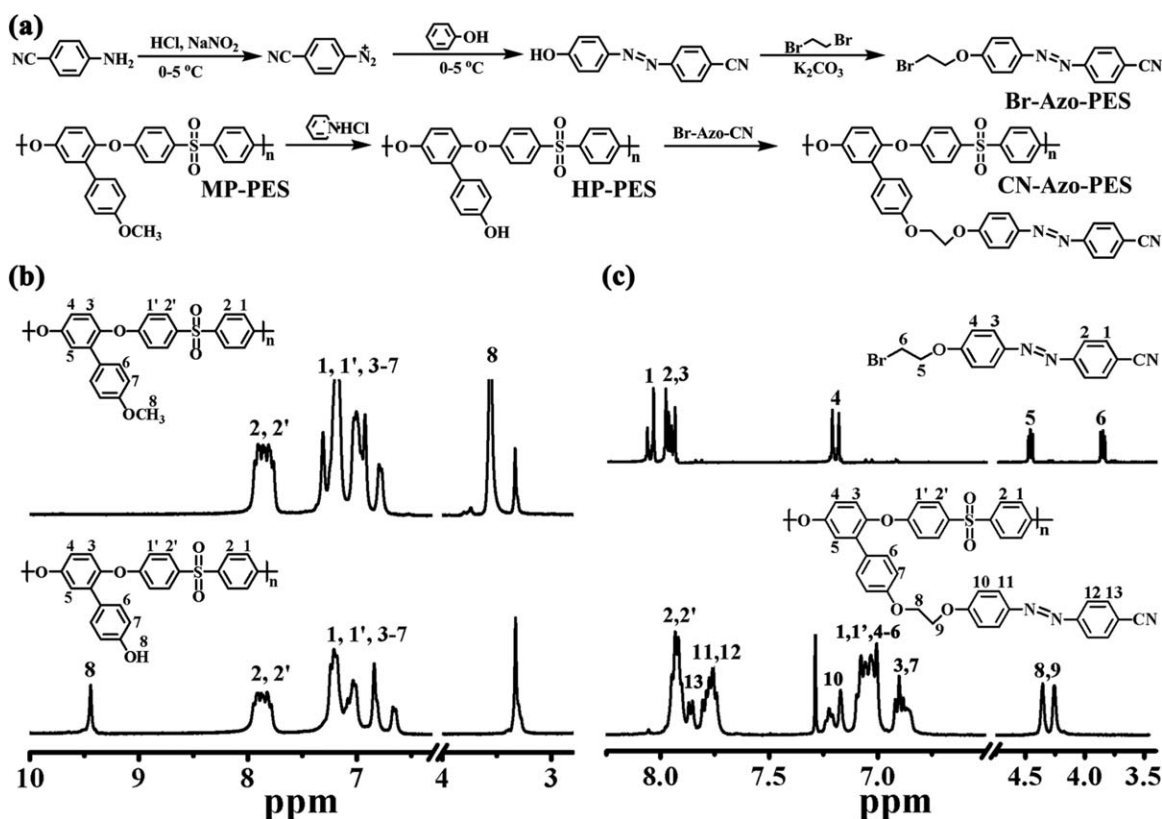


**Figure 1.** (a) The chemical structure and synthesis routes for monomers and polymers; (b) <sup>1</sup>H NMR spectra of polymer MP-PES and HP-PES; (c) <sup>1</sup>H NMR spectra of monomer Br-Azo-CN and polymer CN-Azo-PES.

Polyethersulfone (PES), a cheap but superior engineering thermoplastic, has already been widely used in such fields as proton exchange membranes,<sup>19</sup> oxygen-sensing nanofibers,<sup>20</sup> phase inversion membranes,<sup>21</sup> dielectric materials for printed circuit boards,<sup>22</sup> and many more, owing to its excellent physical, chemical, and dielectric properties. On account of its excellent properties, PES decorated with some functional moieties can meet the requirement for as an active polymer layer in the memory device. At the same time, polymers bearing azobenzene moieties also have now been widely applied in various technological areas, such as in the optical data storage, holographic memories, nonlinear optics, waveguide switches, and other photonic devices because of their high photosensitivity of the azobenzene molecules.<sup>23–25</sup> In particular, the high photosensitivity of the azo dye molecules makes azobenzene polymers popular for use as optical and electronic materials. Also according to the literature, some azobenzene derivatives can be induced by an electric field.<sup>26–32</sup> Kang and his coworkers have demonstrated that polymers bearing pendent azobenzene chromophores with electron-accepting terminal moieties exhibit write-once read-many (WORM) behavior which is attributed to charge trapping at the azobenzene chromophores and that the device has a low onset voltage.<sup>32</sup> Evidently, a low threshold voltage can be beneficial to energy saving and environment protection. All of above have demonstrated the potential of azobenzene-based polymers to function as an active material in the electronic memory device.

In this study, for the same reasons and in order to integrate the high performance of PES with the electrosensitivity of

azobenzene moieties, a novel functional polyethersulfone material bearing pendent azobenzene chromophores (CN-Azo-PES) was designed and synthesized for the application in WORM type memory device, based on the charge-trapping mechanism. With a flexible ethoxyl linkage between the backbone and the side chain, the synthesized material can have the maximum maintenance of the high thermal performance of PES and the electrosensitivity of azobenzene. As was expected, the device exhibits excellent WORM memory behavior with an onset voltage as low as 1.0 V and a current ratio higher than 10<sup>2</sup>. Also the information can be kept for longer than 4 × 10<sup>5</sup> s and read for more than 400 cycles.

## EXPERIMENTAL

### Materials and Methods

Tetramethylene sulfone (TMS) (Jinzhou Oil Refinery), N,N-Dimethylacetamide (DMAc) (Sinopharm Chemical Reagent), and N,N-Dimethylformamide (DMF) (Beijing Chemical Reagent) were purified by distillation under reduced pressure before used and kept with 4 Å molecular sieves. Pyridine hydrochloride was freshly prepared in our lab by distilling water from a certain mixture of pyridine and hydrochloric acid. With (4-methoxy)phenylhydroquinone (MPHQ) and 4,4'-dichlorodiphenyl sulfone (DCDPS) as the monomers, Polyethersulfone bearing methoxy phenyl side groups [MP-PES, see in Figure 1(a)] was synthesized in our lab using according to the literature.<sup>19</sup> All the other commercially available reagents or anhydrous solvents obtained from reagent suppliers (Beijing Chemical Works,

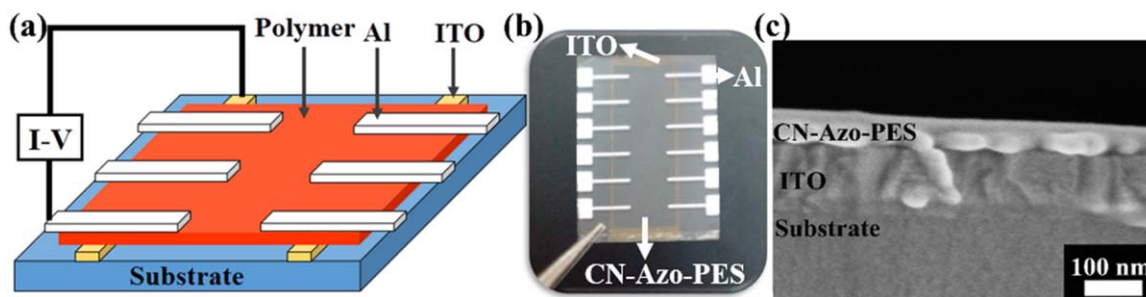


**Figure 2.** (a) The structure of the sandwich-like memory device ITO/polymer/Al; (b) photograph of the memory device designed in this work; (c) SEM image of the cross section for the device. [Color figure can be viewed in the online issue, which is available at [wileyonlinelibrary.com](http://wileyonlinelibrary.com).]

Sinopharm Chemical Reagent or Tianjin Chemical Reagent) were used without further purification unless otherwise noted.

The structures of the monomer and polymers were determined by nuclear magnetic resonance (NMR) spectroscopy (Bruker 510, 500 MHz, DMSO- $d_6$  or  $CDCl_3$  as the solvent and tetramethyl silane as the reference). The weight-average molecular weight ( $M_w$ ) and the corresponding polydispersity index (PDI) of the polymers were obtained by gel permeation chromatography (GPC) on chromatography PL-GPC 220 system (THF as the mobile phase, flow rate of  $1.0 \text{ mL min}^{-1}$ , and polystyrene as the standards). The thermal properties of the polymers were performed by thermogravimetric analysis (TGA) (PerkinElmer TGA-7, heating rate of  $10^\circ\text{C min}^{-1}$  and under an  $N_2$  flow rate of  $50 \text{ mL min}^{-1}$ ) and differential scanning calorimetry (DSC) measurements (Mettler Toledo DSC821e instrument, heating rate of  $10^\circ\text{C min}^{-1}$  under nitrogen atmosphere). UV-vis spectra were acquired on a Shimadzu 3600 UV-vis-NIR spectrophotometer (DMF, THF, DMAc, or  $CHCl_3$  as the solvent). The thickness of the CN-Azo-PES film coated on the ITO substrate was measured using a Veeco Dektak 150 surface profiler. The structure of the memory device was determined by scanning electron microscopy (SEM) (Hitachi, SU8000, gold-coated, HV: 1.5 kV, WD: 2.3 mm). The current-voltage ( $I$ - $V$ ) characteristics of the memory device were recorded by a semiconductor parameter analyzer (Keithley 2400-PR650) in ambient environment at room temperature. A CHI660C Electrochemical Workstation (Shanghai Chenhua Instruments, China) using a three-electrode cell was applied to check the cyclic voltammetry (C-V) property of the polymer under a nitrogen environment. A solution of CN-Azo-PES in THF was coated on a glassy carbon electrode and scanned anodically in a 0.1M acetonitrile solution of tetrabutylammonium perchlorate (TBAP) with  $Ag/Ag^+$  reference electrode and a platinum wire counter electrode.

### Synthesis of Monomers and Polymers

The compounds were prepared as detailed in Figure 1(a).

**Synthesis of Polyethersulfone with Hydroxyl Side Groups (HP-PES).** A mixture of MP-PES (3.00 g) and freshly prepared pyridine hydrochloride (100 g) was heated and stirred at  $170^\circ\text{C}$  until the solution became homogeneous with the protection of nitrogen.<sup>33,34</sup> After being cooled to  $140^\circ\text{C}$ , the mixture was poured into cold water, washed thoroughly, filtered and dried in vacuum. Yield: 2.81 g (96.5%).

**Synthesis of 4-((4-(2-bromoethoxy)phenyl)diazenyl)Benzonitrile (Br-Azo-CN).** The novel monomer was prepared in a three-step synthetic procedure: Firstly, after 4.0 mL HCl (48.0 mmol) being added into 4-aminobenzonitrile (1.42 g, 12.0 mmol) aqueous suspension with vigorous mechanical stirring, the saturated aqueous solution of  $NaNO_2$  (0.84 g, 12.2 mmol) was added dropwise at  $0^\circ\text{C}$ . Then, the resulting yellow solution was added into a mixture of phenol (1.24 g, 13.1 mmol),  $NaHCO_3$  (0.40 g, 4.8 mmol), and  $Na_2CO_3$  (6.00 g, 56.6 mmol) with stirring at  $0^\circ\text{C}$ . It was stirred for 2 hours at that temperature for complete reaction. After that, HCl was added to the reaction mixture to make pH=7. The precipitate was collected and washed thoroughly with water. At last, a mixture of 4-((4-hydroxyphenyl)diazenyl)benzonitrile,  $K_2CO_3$ , and 1,2-dibromoethane in 100 mL acetone was heated to reflux with stirring for 24 hours under  $N_2$  protection. Then, the hot mixture was cooled and filtered. After the removal of solvent, an orange-red powder was collected and purified by silica column chromatography. Yield: 2.89 g (73.0%).  $^1\text{H NMR}$  (500 MHz, DMSO- $d_6$ ,  $\delta$ ): 8.04 (d,  $J = 8.4 \text{ Hz}$ , 2H; Ar-H), 7.94–7.98 (m, 4H; Ar-H), 7.19 (d,  $J = 9.0 \text{ Hz}$ , 2H; Ar-H), 4.47 (t,  $J = 5.4 \text{ Hz}$ , 2H;  $CH_2$ ) 3.86 (t,  $J = 5.4 \text{ Hz}$ , 2H;  $CH_2$ )

**Synthesis of Polyethersulfone with Azobenzene Side Groups (CN-Azo-PES).** The monomer of Br-Azo-CN (0.25 g, 0.75 mmol) and  $K_2CO_3$  (0.25 g) was added to a solution of HP-PES (0.2 g) in dry DMF (6 mL). The mixture was heated at  $100^\circ\text{C}$  for 36 h with the protection of  $N_2$ . Then the mixture was cooled and poured into purified water, washed with water and ethanol, and dried in vacuum at  $100^\circ\text{C}$  for 24 h.

### Fabrication of the Memory Device

As sketched in Figure 2(a,b), the memory device was fabricated with the configuration of indium tin oxide (ITO)/polymer/Al. Firstly, ITO glass was cleaned by ultrasonic with deionized water, acetone, and isopropanol in that order for 15 min each and baked in a vacuum oven at  $80^\circ\text{C}$  overnight to remove the residual solvent. After that, 10 mg/mL solution of CN-Azo-PES in DMF was filtered with microfilters with a pore size of 0.22  $\mu\text{m}$  and spin-coated onto the pre-cleaned ITO glass substrates at speed rates of 3000 rpm for 60 s, and then baked at  $80^\circ\text{C}$  for 12 h under vacuum for the removal of the residual solvent. Lastly, 100 nm-thick Al electrodes were successfully vacuum-deposited on the surface of the polymer layer at  $4 \times 10^{-4} \text{ Pa}$  through a special tailor made shadow mask (slits size: 0.2 mm). Finally, the device owned a structure of ITO/CN-Azo-PES/ Al

**Table I.** The Solubility of Polymer HPPES and CN-Azo-PES in Common Solvents<sup>a</sup>

Solvent	DMF	DMAC	CHCl <sub>3</sub>	THF	DMSO
HP-PES	+	+	+	+	+
CN-Azo-PES	++	++	++	++	++

<sup>a</sup> ++, Soluble at room temperature; +, soluble at heat.

with active areas of 0.2×0.2 mm<sup>2</sup> was obtained to verify the electrical performance.

## RESULTS AND DISCUSSION

### Synthesis and Characterization

As shown in Figure 1(b), HP-PES was successfully prepared from MP-PES. The peak at 3.6 ppm in MP-PES disappeared (-OCH<sub>3</sub>) in the <sup>1</sup>H NMR spectrum of HP-PES, but a new peak at 9.5 ppm (-OH) occurred, indicating that methyl in the polymer side chain was successfully substituted by hydrogen. In order to maintain the high thermal performance of PES and the electro-sensitivity of Azo moieties, CN-Azo-PES was synthesized by a “grafting to” strategy to inoculate the azobenzene moiety to the side chain of PES with a flexible ethoxyl linkage between the polymer backbone and the side chain. By determining the area ratio of the peak at a shift of 7.9 ppm and the peak at a shift of 4.3 ppm in <sup>1</sup>H NMR shown in Figure 1(c), the grafting ratio is higher than 85%. As revealed by GPC measurement, the weight-average molecular weight of CN-Azo-PES is about 35,000, while that of HP-PES is 32,000. The polydispersity index of the former is about 1.53. The successful combination of the two molecules would endow the synthetic polymer with some special properties, in particular, solubility.

As depicted in Table I, HP-PES has poor solubility and only dissolves in hot strong polar solvents for the strong intermolecular and intramolecular hydrogen bonding caused by hydroxy groups in the polymer side chain. On the contrary, the CN-Azo-PES polymer has better solubility in common solvents compared with HP-PES because of the large and relatively flexible side chain in each polymer unit. Moreover, the excellent solubility of CN-Azo-PES will contribute to the device fabrication for various choices of solvents in spin coating process and property measurement of the synthesized polymer.

The UV-visible absorption spectra of the two polymers, HP-PES and CN-Azo-PES, in dilute solutions are shown in Figure 3. The spectrum of HP-PES exhibits only one absorption peak at 275 nm. Unlike HP-PES, however, the spectrum of CN-Azo-PES exhibits two major absorption peaks because of the azobenzene chromophore in the side chain of the polymer. The difference in the absorption wavelength of the two polymer HP-PES and CN-Azo-PES can also be an evidence of the successful combination of PES with azobenzene moieties. And for CN-Azo-PES, the absorption peak at a wavelength of 275 nm (as same as HPPES) is attributed to the  $\pi$ - $\pi^*$  electronic transition of the aromatic ring, while the peak a at the longer wavelength is because of charge transfer (CT) in the azobenzene chromophore caused by the vibronic coupling between  $n$ - $\pi^*$ , and  $\pi$ - $\pi^*$  electronic transitions of the *trans*-azobenzene chromophore.<sup>32,35</sup>

Compared to the absorption peak at lower wavelength, the intensity of peak a is relatively low because of the weak electron-donating characteristic of the ester oxygen between the polymer main chain and the azo side chain. Thus the  $\pi$ -electron delocalization is reduced. Observed from the insert figure in Figure 3, CN-Azo-PES also exhibits a significant positive solvatochromic shift for the lowest energy  $\pi$ - $\pi^*$  transition. With an increase in the solvent polarity of the polymer solution from CHCl<sub>3</sub> to DMAC, the dipolar character of the excited state is enhanced.<sup>32</sup> As a result, an enormous difference is produced in the molecular dipole moment between the electronic ground state and the CT excited state. Accordingly, the red shift in the absorption wavelength in UV-vis spectra can be regarded as an indication of an overall increase in the dipole moment or polarity of the local environment.<sup>36</sup> Hence, CN-Azo-PES has high photosensitivity. Particularly, the high photosensitivity makes it popular as optical and electronic materials. Thus, CN-Azo-PES has great potential as the active layer in the polymer electrical memory device.

### Electrical Switching Behavior

To verify the electrical performance (the current to voltage response, the ON/OFF current ratio, and the threshold voltage), a sandwich-like device owned a structure of ITO/CN-Azo-PES/Al [Figures 2 and 4(b)] is used. The polymer layer thickness was 58 nm detected by surface profiler which coincide with the data by SEM [Figure 2(c)]. And for the device ITO/CN-Azo-PES/Al with an active area of 0.04 mm<sup>2</sup>, as shown in Figure 4(c), the active polymer layer possesses an excellent electrical switching performance.

In the first sweep with a voltage from 0 to -5 V, namely the data “Write” process, at a voltage about -1.0 V (the threshold voltage), the device switched from low-conductivity state (OFF state) to high-conductivity state (ON state) with an abrupt increase in current from 10<sup>-5</sup> to 10<sup>-3</sup> A, which indicated that data were successfully written in the device. While in sweep 2 to

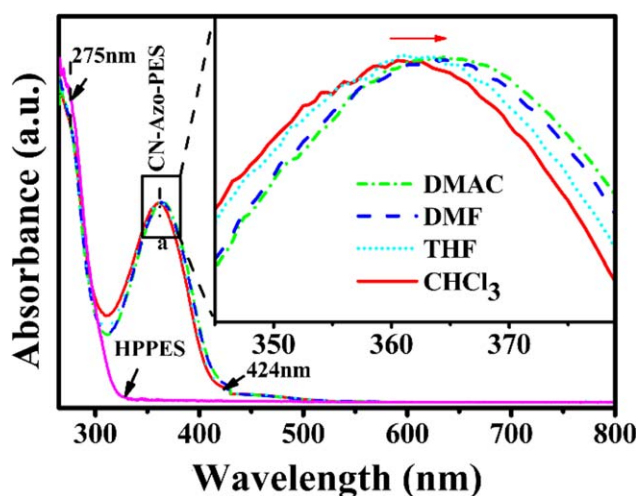


**Figure 3.** The UV-vis spectra of HPPES in DMF and CN-Azo-PES in THF, CHCl<sub>3</sub>, DMAC and DMF, and the spectra in the range of 340 to 380 nm (insert). [Color figure can be viewed in the online issue, which is available at [wileyonlinelibrary.com](http://wileyonlinelibrary.com).]

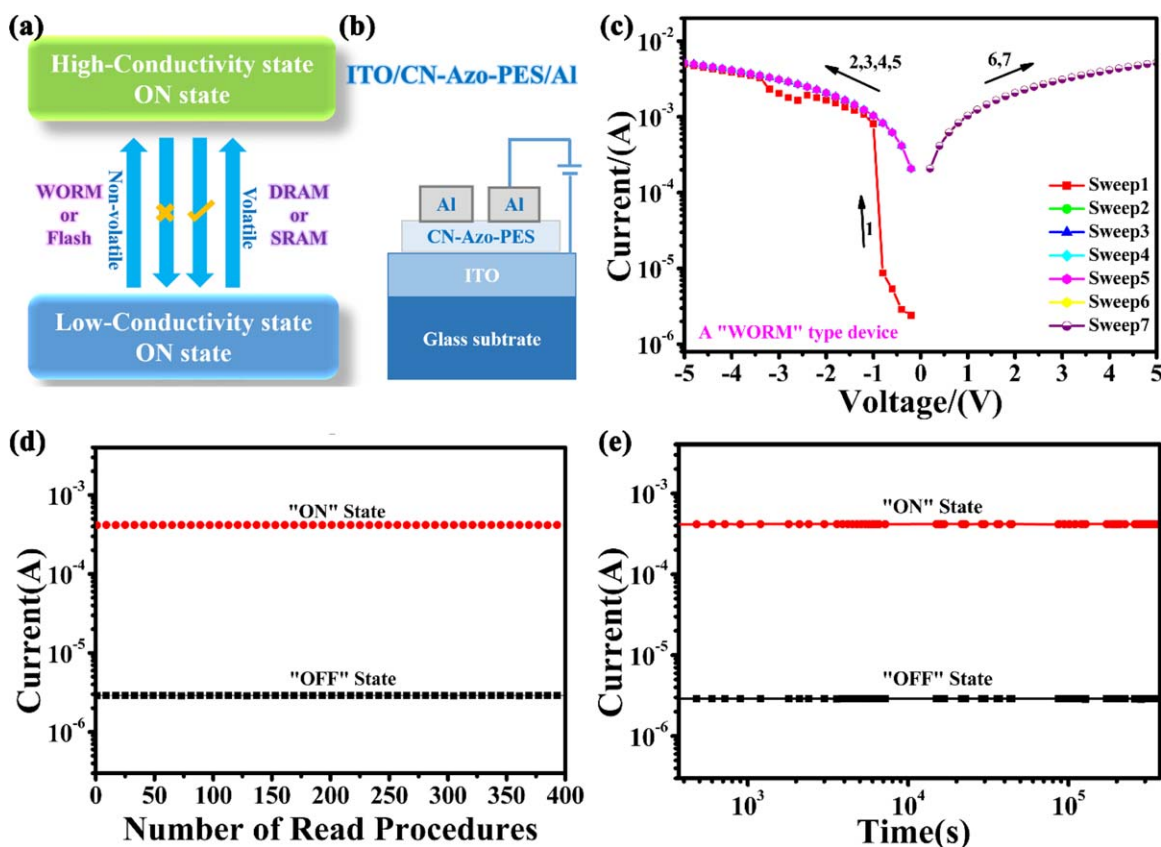


**Figure 4.** (a) The type of memory; (b) the sandwich like memory device structure; (c) the Current–Voltage ( $I$ – $V$ ) characteristics of the device (ITO/CN-Azo-PES/Al) under ambient atmosphere; (d) the read stability for the device under a read voltage of 0.4 V at ambient conditions; (e) the retention time for the ITO/CN-Azo-PES/Al device under a read voltage of 0.4 V. [Color figure can be viewed in the online issue, which is available at [wileyonlinelibrary.com](http://wileyonlinelibrary.com).]

5 (negative bias from 0 to  $-5$  V) and 6 to 7 (positive bias from 0 to 5 V), in other words, the data “Read” process, the current of the device stayed in a relatively high value with no sudden decrease or increase in current. As shown in Figure 4(a), once the low-conductivity state is turned to the high-conductivity state at a certain voltage and the high-conductivity state cannot return to the low-conductivity state by an applied voltage, the device will have a nonvolatile type memory behavior (WORM or Flash). Otherwise, the device will have a volatile type memory behavior (DRAM or SRAM). Thus, according to the above electrical performance, it is believable that the memory device performs a WORM memory behavior as it is both nonrewritable and nonvolatile after it has been once switched to the “ON” state with a ON/OFF current ratio higher than  $10^2$ . And the relative high current ratio will endow the device with two distinguishable state. Unlike volatile type memory (DRAM or SRAM) and nonvolatile rewritable memory (NRWM), the ON state of WORM type memory can be kept and remain nonrewritable for ages once written, which can avoid the miswriting or changing of information in the data reading procedure. Thus, it is meaningful to design such type of memory to record important data and information for hospitals, companies, and many other organizations. Accordingly, CN-Azo-PES-based WORM type memory can be a decent choice in future memory field.

As we all know, today, energy and environmental problems are global issues needed to be solved. For this reason, it is of crucial importance to develop memory device with lower switching-on voltage because the lower the switching-on voltage is, the lower the read voltage will be. As a consequence, it is necessary to figure out that the threshold voltage of the device in this work is just  $-1.0$  V which is quite low compared with recent literatures shown in Table II. On the basis of the onset voltage data presented in Table II, most of the threshold voltages are higher than 1.5 V. Though many materials with memory behavior have been found, it is also arduous to develop the memory material with low onset voltage. Accordingly, the synthesized polymer in this work possesses a great prospect and will be attractive in the data storage field of low-energy-consumption in the future on account of its lower threshold voltage.

#### Memory Behavior of the Device

For an excellent memory device, the memory behavior, i.e., the memory stability, is also as important as the switching behavior. In the memory “Read” process, as shown in Figure 4(d), when a lower voltage of 0.4 V (Read voltage) was applied, the ON state and OFF state were stable up to 400 read cycles with one minute interval between two read cycles at ambient conditions. In addition, the ON/OFF current ratio can be higher than  $10^2$ , and this current ratio at such a low voltage will endow the

**Table II.** The Threshold Voltage and on/off Current Ratio of the Reported Polymers Based on Recent References

Polymer	Thickness (nm)	$V_{\text{onset}}$ (V)	ON/OFF	Type <sup>a</sup>
PStCH-b-P4VP <sup>40</sup>	100	-4.5	$10^3$	WORM
FI-TPA-TCNE <sup>41</sup>	20	-4.2	$10^5$	WORM
CP2 <sup>42</sup>	160±10	-3.0	$10^2$	WORM
PI-NTCDI5 <sup>43</sup>	175-182	-2.8	$10^4$	WORM
PTPA <sub>2</sub> OXD <sub>8</sub> <sup>44</sup>	100-200	+2.5	$10^3$	WORM
HPPS <sup>15</sup>	80	-2.5	$10^5$	SRAM
6F/CzTPA PI <sup>2</sup>	50	-2.0	$10^4$	SRAM
HDAGO <sup>7</sup>	60	+1.5	$10^5$	NRWM
PS-b-PMMA:PCBM <sup>45</sup>	50-60	-1.5	$10^2$	SRAM
GO-PANI <sup>46</sup>	100	-1.3	$10^3$	NRWM
GO-g-PFCz <sup>47</sup>	100	-1.0	$10^2$	NRWM
PPFS <sup>48</sup>	80	-0.5	$10^3$	NRWM
CN-Azo-PES (this work)	58	-1.0	$10^2$	WORM

<sup>a</sup>WORM is for write-once read-many memory, while NRWM is for nonvolatile rewritable memory and SRAM is for volatile static random access memory.

device with two distinguishable electrical states which can avoid the misreading in the “Read” process.

Furthermore, the performance of the memory retention time was investigated. Moreover, the memory retention time property is quite remarkable as well. Presented in Figure 4(e), both the low-conductivity state (OFF state) and the high-conductivity state (ON state) at a reading voltage of 0.4 V can be kept longer than  $4 \times 10^5$  s without any degradation in current which is equal to that of reported materials, suggesting the absence of sample degradation or dielectric breakdown.<sup>32</sup> Simultaneously, the low read voltage can be beneficial to energy conservation and environmental protection on account of its low energy consumption characteristics. Therefore, an exceptional memory device was obtained with a fine memory nature.

### Thermal Properties of the Polymers

As mentioned above, CN-Azo-PES-based memory device exhibits an exceptional memory characteristic. To the best of our knowledge, to achieve an outstanding device performance, excellent thermal properties of the polymer are important and indispensable, which can avoid the degradation in polymer chain in the device operating process.<sup>37</sup> Thus in our work, the thermal properties of the polymer were evaluated by DSC and TGA to explain the excellent memory performance of the CN-Azo-PES-based device.

For electronic devices, to achieve a better performance in the working process, it is of great importance to avoid the phase separation of the device.<sup>37</sup> In this work, the synthetic material, as shown in Figure 5, shows no crystallization and melting peaks, which indicates that CN-Azo-PES is amorphous polymer and will contribute to avoid the crystallization in the storage process for a better stability of the device.<sup>38</sup> For MP-PES with  $T_g$  of 159°C, after the displacement of methyl group by hydrogen atom, there is a great increase in the  $T_g$  of the product (HP-PES,  $T_g$  205°C) because of the great intermolecular and intramolecular interactions caused by hydroxyl groups in the

polymer side chain. And for CN-Azo-PES, because of the relatively flexible chain in the polymer side chain, an evident decrease in the glass transition temperature ( $T_g$ ) of the polymer was detected. However, the  $T_g$  of CN-Azo-PES is still 151°C, and the relatively high  $T_g$  value is good for its applications as active material in polymer electronic devices.

Figure 6 shows the TGA of CN-Azo-PES. The thermal stability of the product is also excellent with an onset decomposition temperature ( $T_d$ , 5% weight loss) of 373°C. And as shown in the DTG curves, the polymers have two main unstable points of 391°C and 446°C because of the degradation of the side chain and the backbone of the polymer respectively, while a tiny weight loss (1%) at a temperature around 150°C was caused by the evaporation of water absorbed on the polymer surface. From all above, the thermal property of CN-Azo-PES is

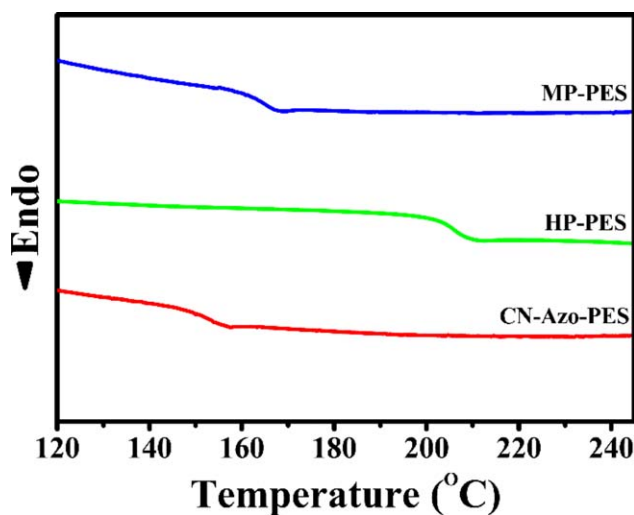


**Figure 5.** The differential scanning calorimetry (DSC) of the three polymers MP-PES, HPPES and CN-Azo-PES. [Color figure can be viewed in the online issue, which is available at [wileyonlinelibrary.com](http://wileyonlinelibrary.com).]

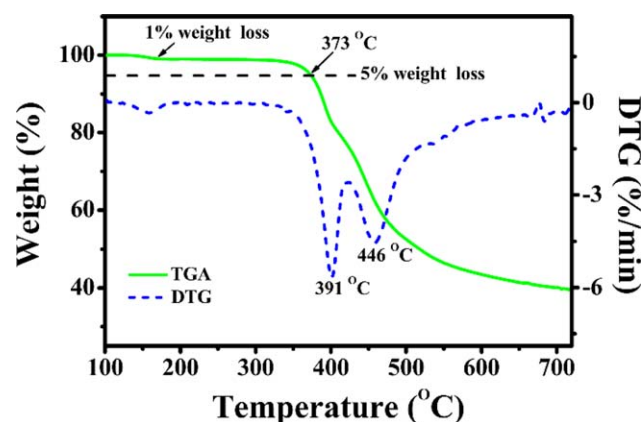


**Figure 6.** The the thermogravimetric analysis (TGA) and DTG curve of CN-Azo-PES. [Color figure can be viewed in the online issue, which is available at [wileyonlinelibrary.com](http://wileyonlinelibrary.com).]

comparable with that of polyimides<sup>3,4,18</sup> and better than the other polymer materials that have been reported for electrical memory usage.<sup>13,26,28,39</sup> And to the best of our knowledge, in the memory storage processes, the outstanding thermal stabilities will make contributions to the performance of the devices for the absence of thermal decomposition. Therefore, the outstanding memory performance of the CN-Azo-PES-based memory device is partially because of the excellent thermal performance.

### The Switching Mechanism

In this study, the CN-Azo-PES-based memory was designed according to the charge-trapping mechanism. To demonstrate the mechanism of CN-Azo-PES-based memory, the orbital values of CN-Azo-PES and UV-vis absorption spectra of CN-Azo-PES film were used.

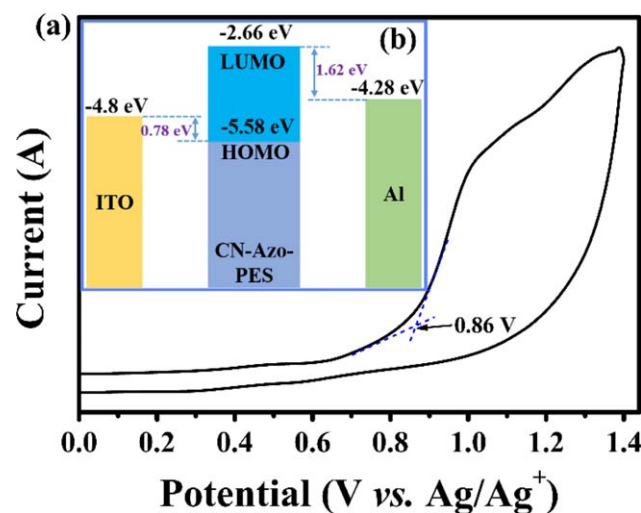


**Figure 7.** (a) The cyclic voltammetry (C-V) curve of CN-Azo-PES coated on a glassy carbon electrode using Ag/Ag<sup>+</sup> reference electrode and a platinum wire counter electrode; (b) the energy level diagram for the device (ITO/CN-Azo-PES/Al). [Color figure can be viewed in the online issue, which is available at [wileyonlinelibrary.com](http://wileyonlinelibrary.com).]

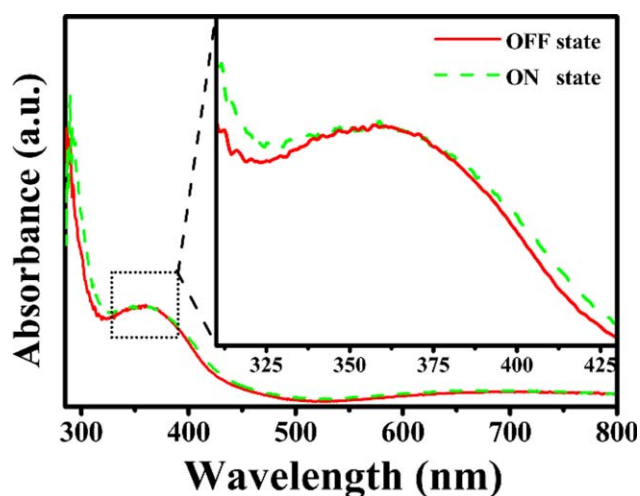


**Figure 8.** Comparison of the UV-visible spectra of the CN-Azo-PES polymer thin film in the low-conductivity (OFF) state and high-conductivity (ON) state. [Color figure can be viewed in the online issue, which is available at [wileyonlinelibrary.com](http://wileyonlinelibrary.com).]

The experimental values of the HOMO (highest occupied molecular orbital) and LUMO (lowest unoccupied molecular orbital) of CN-Azo-PES were obtained by C-V and UV-vis data. CN-Azo-PES has an irreversible oxidation peak at an onset voltage about 0.86 V vs Ag/AgNO<sub>3</sub> as shown in Figure 7(a), which is caused by the irreversible oxidation of the azobenzene moieties in the polymer side chain. Thus, azobenzene chromophore tends to donate electrons and can serve as an efficient hole-transport site.

The HOMO and LUMO energy level can be calculated from the following equations based on the reference energy level of ferrocene which is 4.8 eV below the vacuum level and defined as zero:

$$\text{HOMO} = -[E_{\text{Ox}}(\text{onset}) - E_{\text{Foc}} + 4.8] \text{ eV} \quad (1)$$

$$\text{LUMO} = \text{HOMO} + E_g \quad (2)$$

wherein  $E_{\text{Foc}}$  is the potential of the external standard, i.e., the ferrocene/ferrocenium ion couple (Foc/Foc<sup>+</sup>), which was determined under the same experimental conditions as +0.08 eV vs Ag/AgNO<sub>3</sub>.  $E_{\text{ox}}(\text{onset})$  is +0.86 eV for CN-Azo-PES. Thus, the HOMO energy level is about -5.58 eV relative to the vacuum level. Calculated from the absorption edge of the UV-vis absorption spectrum in Figure 3 which is 424 nm, the band gap  $E_g$  ( $1240/\lambda_{\text{edge}}$ ) was obtained as 2.92 eV related to the HOMO to LUMO transition of CN-Azo-PES, giving a corresponding LUMO energy level of -2.66 eV. When CN-Azo-PES is used as the active layer in the electrical memory device, as shown in Figure 7(b), the energy barrier between HOMO energy level of CN-Azo-PES and  $\Phi$  of ITO (-4.8 eV) is 0.78 eV which is lower than energy barrier (1.62 eV) between LUMO energy level of CN-Azo-PES and  $\Phi$  of Al (-4.28 eV).<sup>26</sup> Thus, CN-Azo-PES is a p-type material. When the device is applied in an electric field, the hole injection from ITO electrode into the HOMO of CN-Azo-PES is more preferable than the electron injection from Al electrode into the LUMO of CN-Azo-PES. Thus, the switching

behavior is ascribed to the charge injection and holes dominate the conduction process.<sup>26</sup>

To further understand the electrical transition from the low-conductivity state to the high-conductivity state in this WORM type memory, UV-vis absorption spectra of CN-Azo-PES polymer thin film before and after applying an electric field were used to verify the difference between the ON state and the OFF state. As illustrated in Figure 8, once the device was turned on, compared with the absorption spectrum of the low conductivity state (OFF state), a slight red shift and broadening of the absorption band of the polymer film have been obtained because of the electric transition. The red shift can be an evidence for an increase in the polarity of the local environment because of an increase of the dipole moment of the azobenzene group. In the solid state as a polymer film, the change can be ascribed to an increase in the dipole moment of the azobenzene chromophore which was caused by the charge trapping and subsequent intramolecular CT in the polymer film during the electrical transition from OFF-to-ON state. For the memory device using azobenzene polymer as the active layer, when the terminal moieties of the azobenzene chromophore are electron acceptors, i.e., cyano group (-CN) in this study, trapped charges can be stabilized by intramolecular CT to form a charge-separated state. Moreover, the filled traps may not be detrapped under reverse fields. As a result, the high-conductivity state (ON state) then can be retained for a long time. All above further clarified that why the OFF to ON transition is permanent and that the memory device could show the WORM type memory behavior.<sup>32</sup>

## CONCLUSIONS

In this study, CN-Azo-PES with the excellent thermal performance of PES and high electro-sensitivity of azobenzene was successfully synthesized for electrical memory usage. A WORM type memory device was obtained by CN-Azo-PES as the active layer with a structure of ITO/CN-Azo-PES/Al. For the memory device, the threshold voltage is as low as  $-1.0$  V with an ON/OFF current ratio higher than  $10^2$ . Moreover, when a  $0.4$  V read voltage was applied, the device can even endure 400 reading cycles and the memory can be maintained for more than  $4 \times 10^5$  s because of the excellent thermal performance of CN-Azo-PES. The WORM type memory can be explained by charge-trapping mechanism of hole injection. Consequently, an outstanding memory device was obtained with a distinguished memory characteristic. Therefore, CN-Azo-PES is appealing as an advanced polymer memory material in the field of low power consumption memory in the future on account of its low threshold voltage as well as the excellent data maintaining performance.

## ACKNOWLEDGMENTS

This work was financially supported by the Science and Technology Department of Jilin Province Foundation (20130204026GX). Also the authors express their great thanks for the kindly support Prof. Yue Wang and Dr. Kai Wang from the state key laboratory of supramolecular structure and materials (Jilin University, Changchun) in the device fabrication process.

## REFERENCES

1. Ling, Q.-D.; Liaw, D.-J.; Zhu, C.; Chan, D. S.-H.; Kang, E.-T.; Neoh, K.-G. *Prog. Polym. Sci.* **2008**, *33*, 917.
2. Shi, L.; Tian, G.; Ye, H.; Qi, S.; Wu, D. *Polymer* **2014**, *55*, 1150.
3. Li, Y. Q.; Chu, Y. Y.; Fang, R. C.; Ding, S. J.; Wang, Y. L.; Shen, Y. Z.; Zheng, A. M. *Polymer* **2012**, *53*, 229.
4. Yu, A. D.; Kurosawa, T.; Lai, Y. C.; Higashihara, T.; Ueda, M.; Liu, C. L.; Chen, W. C. *J. Mater. Chem.* **2012**, *22*, 20754.
5. Kuorosawa, T.; Chueh, C.-C.; Liu, C.-L.; Higashihara, T.; Ueda, M.; Chen, W.-C. *Macromolecules* **2010**, *43*, 1236.
6. Zhuang, X.; Chen, Y.; Wang, L.; Neoh, K.-G.; Kang, E.-T.; Wang, C. *Polym. Chem.* **2014**, *5*, 2010.
7. Zhang, L.; Li, Y.; Shi, J.; Shi, G.; Cao, S. *Mater. Chem. Phys.* **2013**, *142*, 626.
8. Zhang, Q.; Pan, J.; Yi, X.; Li, L.; Shang, S. M. *Org. Electron.* **2012**, *13*, 1289.
9. Onlaor, K.; Thiwawong, T.; Tunhoo, B. *Org. Electron.* **2014**, *15*, 1254.
10. Bae, S.-k.; Lee, S.-Y.; Hong, S. C. *React. Funct. Polym.* **2011**, *71*, 187.
11. Liu, J. Q.; Zeng, Z. Y.; Cao, X. H.; Lu, G.; Wang, L. H.; Fan, Q. L.; Huang, W.; Zhang, H. *Small* **2012**, *8*, 3517.
12. Lai, Y.-S.; Tu, C.-H.; Kwong, D.-L.; Chen, J. S. *Appl. Phys. Lett.* **2005**, *87*, 122101.
13. Lee, T. J.; Park, S.; Hahm, S. G.; Kim, D. M.; Kim, K.; Kim, J.; Kwon, W.; Kim, Y.; Chang, T.; Ree, M. *J. Phys. Chem. C* **2009**, *113*, 3855.
14. Jha, P.; Koiry, S. P.; Saxena, V.; Veerender, P.; Gusain, A.; Chauhan, A. K.; Aswal, D. K.; Gupta, S. K. *Org. Electron.* **2013**, *14*, 2896.
15. Lu, C.; Liu, Q.; Gu, P.; Chen, D.; Zhou, F.; Li, H.; Xu, Q.; Lu, J. *Polym. Chem.* **2014**, *5*, 2602.
16. Yang, Y.; Ouyang, J.; Ma, L.; Tseng, R. J. H.; Chu, C. W. *Adv. Funct. Mater.* **2006**, *16*, 1001.
17. Ling, Q. D.; Chang, F. C.; Song, Y.; Zhu, C. X.; Liaw, D. J.; Chan, D. S.; Kang, E. T.; Neoh, K. G. *J. Am. Chem. Soc.* **2006**, *128*, 8732.
18. Liu, Y.-L.; Ling, Q.-D.; Kang, E.-T.; Neoh, K.-G.; Liaw, D.-J.; Wang, K.-L.; Liou, W.-T.; Zhu, C.-X.; Chan, D. S.-H. *J. Appl. Phys.* **2009**, *105*, 044501.
19. Guo, M.; Li, X.; Li, L.; Yu, Y.; Song, Y.; Liu, B.; Jiang, Z. *J. Membr. Sci.* **2011**, *380*, 171.
20. Xue, R.; Behera, P.; Viapiano, M. S.; Lannutti, J. *J. Mater. Sci. Eng. C* **2013**, *33*, 3450.
21. Sadrzadeh, M.; Bhattacharjee, S. *J. Membr. Sci.* **2013**, *441*, 31.
22. Apeldorn, T.; Keilholz, C.; Wolff-Fabris, F.; Altstädt, V. *J. Appl. Polym. Sci.* **2013**, *128*, 3758.
23. Sun, W.; He, X.; Liao, X.; Lin, S.; Huang, W.; Xie, M. *J. Appl. Polym. Sci.* **2013**, *130*, 2165.
24. Yamada, H.; Kukino, M.; Wang, Z. A.; Miyabara, R.; Fujimoto, N.; Kuwabara, J.; Matsuishi, K.; Kanbara, T. *J. Appl. Polym. Sci.* **2015**, 132.



25. Zhao, F.; Wang, C.; Zeng, Y.; Zhang, J. *J. Appl. Polym. Sci.* **2013**, *130*, 406.
26. Li, H.; Lu, J.; Li, N.; Xu, Q.; Ge, J.; Wang, L.; Luan, Z. *Sci. Chin. Chem.* **2010**, *53*, 588.
27. Bandyopadhyay, A.; Sahu, S.; Higuchi, M. *J. Am. Chem. Soc.* **2011**, *133*, 1168.
28. Zhuang, H.; Xu, X.; Liu, Y.; Zhou, Q.; Xu, X.; Li, H.; Xu, Q.; Li, N.; Lu, J.; Wang, L. *J. Phys. Chem. C* **2012**, *116*, 25546.
29. Zhang, Y. H.; Zhuang, H.; Yang, Y.; Xu, X. F.; Bao, Q.; Li, N. J.; Li, H.; Xu, Q. E.; Lu, J. M.; Wang, L. H. *J. Phys. Chem. C* **2012**, *116*, 22832.
30. Liu, G.; Zhang, B.; Chen, Y.; Zhu, C.-X.; Zeng, L.; Chan, D. S.-H.; Neoh, K.-G.; Chen, J.; Kang, E.-T. *J. Mater. Chem.* **2011**, *21*, 6027.
31. Chen, W.; Li, H.; Li, N. J.; Xu, Q. F.; Lu, J. M.; Wang, L. H. *Dyes Pigm.* **2012**, *95*, 365.
32. Lim, S. L.; Li, N. J.; Lu, J. M.; Ling, Q. D.; Zhu, C. X.; Kang, E. T.; Neoh, K. G. *ACS Appl. Mater. Interfaces* **2009**, *1*, 60.
33. Yue, X.; Zhang, H.; Chen, W.; Wang, Y.; Zhang, S.; Wang, G.; Jiang, Z. *Polymer* **2007**, *48*, 4715.
34. Wei, W.; Zhang, H.; Guan, S.; Jiang, Z.; Yue, X. *Polymer* **2012**, *53*, 5002.
35. Cojocariu, C.; Rochon, P. *Macromolecules* **2005**, *38*, 9526.
36. Bartkowiak, W.; Lipiński, J. *J. Phys. Chem. A* **1998**, *102*, 5236.
37. Chuang, C.-N.; Chuang, H.-J.; Wang, Y.-X.; Chen, S.-H.; Huang, J.-J.; Leung, M.-K.; Hsieh, K.-H. *Polymer* **2012**, *53*, 4983.
38. Thelakkat, M. *Macromol. Mater. Eng.* **2002**, *287*, 442.
39. Zhang, B.; Chen, Y. J.; Zhang, Y. F.; Chen, X. D.; Chi, Z. G.; Yang, J.; Ou, J. M.; Zhang, M. Q.; Li, D. H.; Wang, D.; Liu, M. K.; Zhou, J. Y. *Phys. Chem. Chem. Phys.* **2012**, *14*, 4640.
40. Liu, J.; Gu, P.; Zhou, F.; Xu, Q.; Lu, J.; Li, H.; Wang, L. *J. Mater. Chem. C* **2013**, *1*, 3947.
41. Ko, Y.-G.; Kim, D. M.; Kim, K.; Jung, S.; Wi, D.; Michinobu, T.; Ree, M. *ACS Appl. Mater. Interfaces* **2014**, *6*, 8415.
42. Yen, H.-J.; Tsai, H.; Kuo, C.-Y.; Nie, W.; Mohite, A. D.; Gupta, G.; Wang, J.; Wu, J.-H.; Liou, G.-S.; Wang, H.-L. *J. Mater. Chem. C* **2014**, *2*, 4374.
43. Kurosawa, T.; Lai, Y.-C.; Yu, A.-D.; Wu, H.-C.; Higashihara, T.; Ueda, M.; Chen, W.-C. *J. Polym. Sci. A: Polym. Chem.* **2013**, *51*, 1348.
44. Wang, K.-L.; Liu, G.; Chen, P.-H.; Pan, L.; Tsai, H.-L. *Org. Electron.* **2014**, *15*, 322.
45. Jo, H.; Ko, J.; Lim, J. A.; Chang, H. J.; Kim, Y. S. *Macromol. Rapid Commun.* **2013**, *34*, 355.
46. Zhang, B.; Chen, Y.; Ren, Y.; Xu, L.-Q.; Liu, G.; Kang, E.-T.; Wang, C.; Zhu, C.-X.; Neoh, K.-G. *Chem. Eur. J.* **2013**, *19*, 6265.
47. Xu, L. Q.; Zhang, B.; Chen, Y.; Neoh, K.-G.; Kang, E.-T.; Fu, G. D. *Macromol. Rapid Commun.* **2013**, *34*, 234.
48. Yin, C.-R.; Han, Y.; Li, L.; Ye, S.-H.; Mao, W.-W.; Yi, M.-D.; Ling, H.-F.; Xie, L.-H.; Zhang, G.-W.; Huang, W. *Polym. Chem.* **2013**, *4*, 2540.